CHEMICAL SENSORS BASED ON ISFET TRANSDUCERS

A. Lui, B. Margesin, M. Zen
Divisione Microsensori ed Integrazione di Sistema
38050 Povo (TN), Italy

G. Soncini, G. Verzellesi
Dipartimento di Ingegneria dei Materiali,
Universita di Trento, 38050 Mesiano (TN), Italy

INVITED PAPER
24th International Conference on Microelectronics, MIEL'96
32nd Symposium on Devices and Materials, SD'96
September 25.-September 27., 1996, Nova Gorica, Slovenia

Key words: microelectronics, chemical sensors, biochemical sensors, ISFET sensors, ISFET transistors, MOSFET transistors, theoretical fundamentals, semiconductor modelling, computer modelling, EIS capacitors, Electrolyte-Insulator-Semiconductor capacitors, fabrication technologies, electrochemical parameters, ion-sensitive, ion selectivity, ISFET-CMOS processes

Abstract: In this paper, we address the increasingly important and rapidly developing field of ISFET-based silicon integrated biochemical sensors. ISFET transduction mechanism, modelling and electrochemical characterization techniques are reviewed. ISFET fabrication technology, mainly with reference to the ISFET-CMOS process developed at IRST, is described. Two examples of ISFET-based systems for application in the environmental monitoring field are presented.

Kemični senzorji na osnovi ISFET pretvornikov

Ključne besede: mikroelektronika, senzorji kemijski, senzorji biokemijski, ISFET senzorji, ISFET transistorji, MOSFET transistorji, osnove teoretične, modeliranje polprevodnikov, modeliranje računalniško, EIS kondenzatorji elektrolit-izolator-polprevodnik, tehnologije proizvodnje, parametri elektrokemijski, občutljivost na ione, selektivnost za ione, ISFET-CMOS procesi

Povzetek: V prispevku opisujemo vse bolj pomembno in hitro se razvijajoče področje biokemičnih senzorjev na osnovi integriranih ISFET tranzistorjev na siliciju. Podamo mehanizme pretvorbe ISFET tranzistorjev, modeliranje in tehnike elektrokemične karakterizacije komponent. Ravno tako opišemo tehnologijo izdelave teh pretvornikov, kjer kot osnovo vzamemo ISFET-CMOS proces, ki smo ga razvili na IRST. Na koncu predstavimo dva primera uporabe senzorjev na osnovi ISFET pretvornikov pri nadzoru okolja.

1. INTRODUCTION

A chemical sensor is a device which is capable of converting a chemical quantity into an electrical signal. Chemical species to be detected are usually present in mixtures where the sample matrix might be gas, liquid or solid. For instance, a chemical sensor may be required to detect the presence of hydrogen in air (gas sensor), the presence of water vapour in air (humidity sensor) or the presence of ions in water (ion-sensitive sensor). A chemical sensor may also be requested to detect the presence of more complex molecules such as sugar or proteins in a liquid. A chemical sensor designed to detect a biological quantity is usually referred to as a biochemical sensor or biosensor. The different types of chemical sensors can be classified according to the sensing principle by which they detect the chemical measurand. For example, the interaction of a chemical species X with the sensing material M can usually be described by the following reaction:

$$X + M \rightleftarrows_{k_r}^{k_f} XM,$$

where k_f and k_r are the forward and reverse reaction-rate constants. When the reaction liberates (or abstracts) heat due to a change in enthalpy, this can be detected calorimetrically. Alternatively, when the reaction is accomplished by liberation (or abstraction) of electrical charges, this can be detected conductimetrically, amperometrically, or potentiometrically. Selectivity, i.e. the capability to detect only the chemical species X among the many different ones usually present in the sample matrix, depends upon the nature of the reaction mechanism. Selectivity can be enhanced by selecting an active material M which reacts preferentially with the measurand X. Thin or thick layers of these active materials, eventually associated with some filtering action, can be coupled with suitable transducers to develop selective biochemical sensors.

This paper will focus on and discuss only potentiometric biochemical sensors based on the Ion-Sensitive Field-Effect Transistor (ISFET) /1, 2/. This choice is motivated by the following considerations. (i) An ISFET can be considered as a transconductance amplifier that transform an input voltage (high input impedance) to an output current (low input impedence). Therefore, ISFET-type potentiometric sensors do not draw any significant input current and the output signal is much less susceptible to noise. (ii) ISFET's lend themselves to low-cost mass production by using the well established silicon planar technology. (iii) ISFET's can be made compatible, with some limitations, with conventional CMOS processing, which allows smart sensors to be designed and fabricated.

The paper is organized as follows. ISFET theory and modelling are reviewed in Section 2, while fabrication technology is described in Section 3 with emphasis on the ISFET-CMOS fabrication process developed and currently in use at IRST (Trento, Italy). Section 4 is devoted reliability issues, mainly related to selective membrane deposition and device encapsulation and packaging. Finally, among the large variety of possible application of ISFET-based (bio)chemical sensors, only the increasingly important environmental monitoring field will be briefly addressed in Section 5, where two examples of applications recently developed at IRST are presented.

2. ISFET THEORY AND MODELLING

In this section, the operation of the ISFET is first outlined by comparing it to that of a MOSFET. Then, the theory of Electrolyte-Insulator-Semiconductor (EIS) systems is reviewed, and the chemico-physical phenomena underlying the ISFET transduction mechanism are described in more detail. Finally, a simulation technique is briefly described, aiming at a detailed, device-level analysis of pH-ISFET's.

2.1 ISFET vs. MOSFET

The operation of the ion-sensitive field-effect transistor can be best explained by comparing it to that of a conventional Metal-Oxide-Semiconductor Field-Effect Transistor (MOSFET).

As shown in Fig. 1, the ISFET can be viewed as a MOSFET in which the gate metal is replaced by an electrolytic solution with a reference electrode immersed into it. The sequence of contacting phases in the two devices is as follows:

- MOSFET: metal / silicon dioxide / silicon / metal
- ISFET: metal / Ag / AgCl / saturated KCl / test solution / pH-sensitive insulator / silicon dioxide / silicon / metal

where an Ag/AgCl electrode has been assumed as reference electrode for the ISFET. Moreover, the simplest case of ISFET has been considered (and will also be assumed in the following, unless otherwise stated), namely an H^+-sensitive ISFET. To make the device sensitive to other ionic species, specific polymeric membranes can be deposited on top of the gate insulator /3/. As can be seen, when transforming a MOSFET into an ISFET, the interface between metal gate and insulator is to be replaced by a number of additional phases representing the reference electrode, the solution under test, and the pH-sensitive insulating layer. Correspondingly, the ISFET threshold voltage, V_T^*, defined as the externally applied V_{GS} voltage required to bring the silicon surface to the onset of strong inversion, can be deduced from that of the MOSFET, V_T, by simply adding the potential drops at the additional interfaces /4/:

$$V_T^* = V_T + E_{ref} + \varphi_{lj} + \chi_e - \Psi_0(pH) - \varphi_m / q . \qquad (1)$$

In the above equation, E_{ref} is the reference electrode absolute potential, φ_{lj} is the liquid junction potential difference between the reference solution and the electrolyte under test, χ_e is the electrolyte-insulator surface dipole potential, φ_m /q is the work function of the gate metal relative to vacuum. $\Psi_0(pH)$ represents the potential difference between the insulator surface exposed to the electrolyte and the bulk of the electrolyte itself, and is actually the sole pH-dependent term in the ISFET threshold voltage.

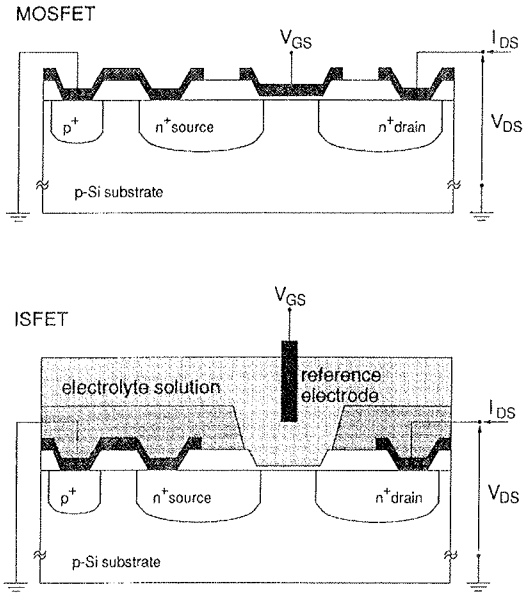

Fig. 1: Schematic cross-sectional view of a MOSFET compared with that of an ISFET.

Once the threshold voltage is known, the current flowing from source to drain in an ISFET can formally be expressed, as a function of the applied voltages, exactly in the same way as in a MOSFET, i.e.:

$$I_{DS} = \begin{cases} K\left[\left(V_{GS} - V_T^*\right) - \left(V_{DS} / 2\right)\right]V_{DS} & \text{for } V_{DS} < V_{GS} - V_T^* \\ K / 2\left(V_{GS} - V_T^*\right)^2 , & \text{for } V_{DS} > V_{GS} - V_T^* \end{cases} \qquad (2)$$

where the conduction factor K is given by $K = \mu_n C_i W/L$, μ_n being the electron (for an n-channel device) mobility, C_i the insulator capacitance per unit area, W and L the channel width and length, respectively.

In the next section, the term Y0(pH) of the ISFET threshold voltage will be shown to be correlated to the surface chemical reactions occurring at the electrolyte-insulator interface. Already at this point of the discussion, however, it is possible to understand the operating principle of the ISFET as a pH sensor: any chemically-induced change in one of the terms at the right-hand side of eqn. 1 shifts, in fact, the threshold voltage of the device, inducing a corresponding change in the device current which can be detected and monitored. To this purpose, ISFET's are normally operated at constant I_{DS} and V_{DS}, i.e. using a feedback circuit, as that depicted in Fig. 2, which compensates for induced changes in I_{DS} by adjusting V_{GS}. The device is commonly biased in the linear part of the triode region (i.e. with $V_{DS} << V_{GS} - V_T^*$), where the drain current, written by neglecting the non-linear term, is simply given by

$$I_{DS} \cong K\left(V_{GS} - V_T^*\right)V_{DS} \quad . \tag{3}$$

Combining eqns. 3 and 1 yields:

$$V_{GS} \cong I_{DS} / (KV_{DS}) + V_T + E_{ref} + \varphi_{lj} + \chi_e - \Psi_0(pH) - \varphi_m / q \,, \tag{4}$$

which, for I_{DS} and V_{DS} held constant, can be written as:

$$V_{GS} \cong const. - \Psi_0(pH) \,. \tag{5}$$

The term denoted as "const." in the above equation summarizes all the quantities at the right-hand side of eqn. 4 which are unaffected by a change in the solution pH. It is evident from eqn. 5 that any change in the electrolyte pH will induce a corresponding change in the gate voltage V_{GS}. This latter can therefore be assumed as the pH-dependent output voltage of the circuit shown in Fig. 2.

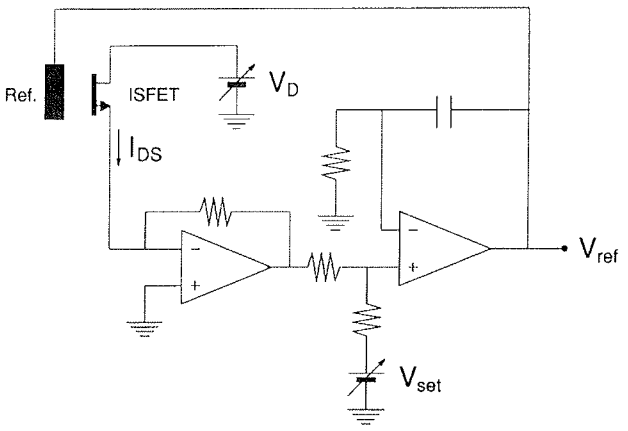

Fig. 2: Sketch of a feedback circuit for measuring pH sensitivity in ISFET devices.

2.2 THE ELECTROLYTE-INSULATOR-SEMICONDUCTOR SYSTEM

ISFET transduction mechanism relies on the properties of the Electrolyte-Insulator-Semiconductor (EIS) capacitor forming the gate structure of the device.

The response of EIS systems to changes in the electrolyte proton concentration is commonly explained by invoking the so-called *site-binding* theory /5/, to describe the physico-chemical processes occurring at the electrolyte-insulator (EI) interface /4, 6 - 10/. According to this theory, the presence of ion-specific binding sites at the surface of the insulator exposed to the electrolyte is responsible for the development of an ion-charge layer on the insulator surface, as a result of chemical reactions between binding sites and H^+ ions. In addition, other ions present in the solution (for instance, Na^+ and Cl^- in a typical univalent electrolyte) can form ion pairs with the charged surface sites. The electrical double layer developing at the electrolyte-solid interface is then completed by a diffuse charge layer formed by the hydrated electrolyte ions. A schematic picture of the charge density distribution throughout the EIS system is given in Fig. 3(a), where σ_0, σ_β, and σ_d represent the charge densities associated with surface sites, counterions, and diffuse layer, respectively. Figure 3(b) shows the corresponding electrostatic-potential distribution. The Outer Helmholtz Plane (OHP) is the locus of the centers of the hydrated ions forming the diffuse layer with the closest approach to the solid, while the Inner Helmholtz Plane (IHP) is the plane of the adsorbed ions which form pairs with the charged surface sites.

In an EIS structure having Si_3N_4 as dielectric material exposed to the electrolyte, silanol sites, as well as primary, secondary, and tertiary amine sites, are present on the Si_3N_4 after oxidation. Neglecting the contribution of secondary and tertiary amine sites, the charge density σ_0 due to surface sites can be expressed as /4/ (similar expressions hold also for different insulating materials):

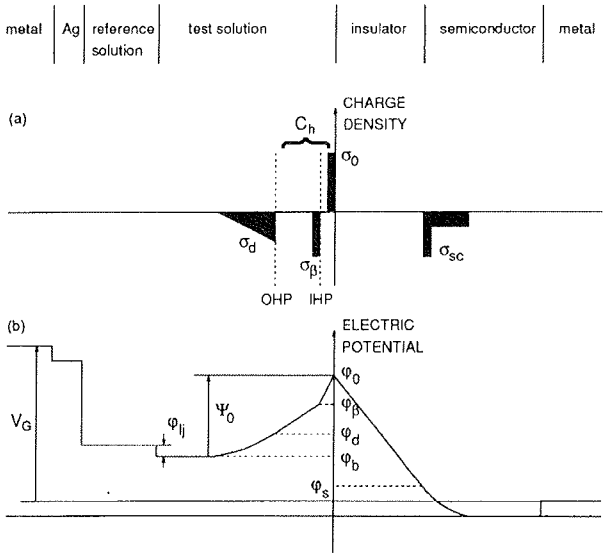

Fig. 3: Sketch of the charge-density (a) and electric-potential (b) distributions in an EIS structure.

$$\sigma_0 = q\left(\frac{[H^+]_s^2 - K_+K_-}{[H^+]_s^2 + K_+[H^+]_s + K_+K_-}\right)N_{sil} + \tag{6}$$

$$+q\left(\frac{[H^+]_s}{[H^+]_s + K_{N+}}\right)N_{nit}.$$

In the above equation, N_{sil} and N_{nit} are the silanol and primary amine binding-site density, respectively, whereas K_+ , K_- and K_{N+} represent the dissociation constants of the surface chemical reactions involving binding sites and H^+ ions. $[H^+]_S$ represents the proton concentration at the EI interface, which is related to that assumed in the electrolyte bulk $[H^+]_b = 10^{-pH}$ through the Boltzmann equation:

$$[H^+]_s = [H^+]_b \, exp[-q(\varphi_0 - \varphi_b)/(kT)], \tag{7}$$

where φ_0 and φ_b are the electrostatic potential at the EI interface and in the electrolyte bulk, respectively. The diffuse layer is governed by the Gouy-Chapman-Stern theory, which dictates that the charge in a column of unit cross-sectional area extending from the OHP to the electrolyte bulk is given by /6, 8/:

$$\sigma_d = \sqrt{8\varepsilon_w kTc_0}\,\sinh\left[\frac{q(\varphi_b - \varphi_d)}{2kT}\right], \tag{8}$$

where φ_d is the potential at the OHP, c_0 is the ion concentration of the solution, and ε_w is the solution permittivity. Neglecting the counterion charge (σ_β) at the IHP, φ_d is related to φ_0 by the Gauss law applied to the electrolyte region extending from the EI interface to the OHP:

$$\varphi_d = \varphi_0 + \frac{\sigma_d}{C_h}, \tag{9}$$

C_h being the capacitance per unit area of the complete Helmoltz layer.

To complete the EIS model, additional equations are needed, defining the charge distribution in the solid-state part of the structure. From the MOS-capacitor theory, one can express the semiconductor charge density, σ_{SC}, as a function of the sole electrostatic potential at the insulator-semiconductor interface, φ_S:

$$\sigma_{sc} = \pm\sqrt{2\varepsilon kTp_{p0}}\left[\left(\frac{q\varphi_s}{kT} - 1 + exp\left(\frac{q\varphi_s}{kT}\right)\right) + \right. \tag{10}$$

$$\left. + \frac{n_{p0}}{p_{p0}}\left(\frac{q\varphi_s}{kT} - 1 + exp\left(\frac{q\varphi_s}{kT}\right)\right)\right]^{1/2}.$$

In the above equation, ε_S is the semiconductor permittivity, n_{p0} and p_{p0} are the equilibrium concentrations of electrons and holes, respectively, and the sign plus applies to the case of $\varphi_S<0$, the minus to the case of $\varphi_S>0$. Moreover, the Gauss law applied to the insulator region yields:

$$\sigma_{sc} = C_i(\varphi_s - \varphi_0). \tag{11}$$

Finally, the charge neutrality for the whole EIS system requires that:

$$\sigma_0 + \sigma_d + \sigma_{sc} = 0, \tag{12}$$

where charges in the oxide and at the Si-SiO_2 interface have been neglected for simplicity.

Equations 6 to 12 can be assumed as the EIS system model. From a mathematical point of view, they form a system of seven equations, which, for instance, can be solved for the following seven unknowns: σ_0, $[H^+]_S$, σ_d, σ_{SC}, φ_0, φ_d, and φ_S, having assumed $[H^+]_b=10^{-pH}$ and φ_b (which differs from the externally applied gate voltage by a constant) as externally defined parameters. So doing, the charge and potential distribution in the whole EIS structure can be calculated for any given value of the solution pH and of the externally-applied gate voltage. Alternatively, system 6-12 can be solved with φ_b unknown and φ_S set to the value of $2\phi_F$ (ϕ_F being the Fermi potential in the semiconductor region), that is, to the onset of strong inversion condition at the semiconductor-insulator interface. In this case, the quantity $\Psi_0=\varphi_0-\varphi_b$, which enters into the ISFET threshold voltage expression (see eqn. 1), can be computed as a function of the solution pH.

2.3 DEVICE-LEVEL SIMULATION

Efforts aimed at making the ISFET fabrication process compatible with CMOS techologies are in progress, to allow chemical sensors and signal-conditioning electronics to be integrated on the same chip. This fact, while opening the way to the development of chemical

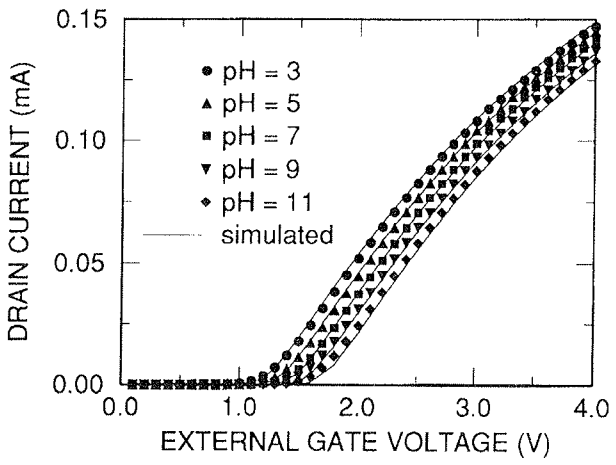

Fig. 4: ISFET transfer characteristics at different pH and V_{DS}=0.1 V.

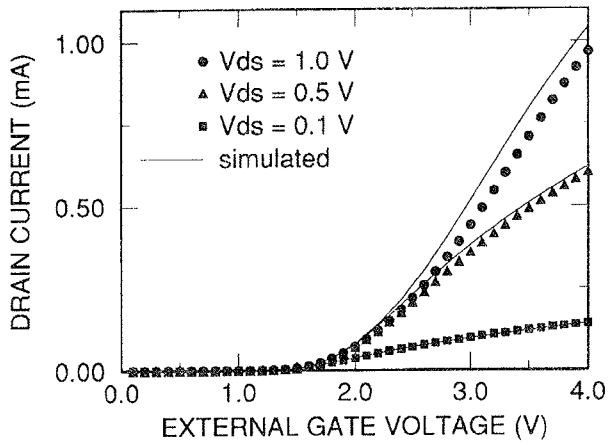

Fig. 5: ISFET transfer characteristics at different drain voltages and pH=7.

smart sensors, imposes that suitable CAD tools be adopted to efficiently and reliably design ion-sensitive IC's. To meet this need, a SPICE model has, for instance, been proposed in /4/. When dealing with the development of ISFET devices and the optimization of fabrication processes, however, a more straightforward relationship between process parameters and device electrical responses is desirable, with respect to that allowed by compact, circuit-simulation-oriented models. This can be achieved by means of device-level simulation. In the following, a technique is briefly described, which allows for the device-level analysis of pH ISFET's. Full account of the simulation technique, as well as of its experimental validation, can be found elsewhere /11, 12/. In this approach, the ion-charge build-up model given by eqns. 6-9 is incorporated into the 2D device-simulator HFIELDS /13/. Such a program solves the fundamental device equations, i.e. Poisson and carrier-continuity equations for electrons and holes, supplemented by the drift-diffusion expressions for the electron and hole current densities. Numerical solution of these equations is carried out by discretizing them on a 2D triangular grid. To the purpose of linking eqns. 6-9 to the semiconductor-device model, a gradual approximation is assumed to hold within the electrolyte, i.e., the potential at the electrolyte-insulator interface is assumed to vary slowly along the direction parallel to the insulator surface. This allows for the adoption of a 1D, lumped model of the charge distribution in the electrolyte along the direction normal to the same surface. Equations 6-9 are then coupled with Poisson's equation and solved at each element of the discretized electrolyte-insulator interface, thus providing a self-consistent description of the charge and potential distribution within the whole EIS system. By this approach, technological details such as the actual doping profile, specific geometries, surface defects, oxide-trapped charge, etc., can easily be taken into account and the TCAD optimization of the ISFET device and fabrication process is made feasible.

To validate the implemented models, the HFIELDS program equipped with the new capability has been employed to simulate ISFET's fabricated at IRST with a CMOS-compatible technology, whose main features are described in the next section. Computed characteristics have, then, been compared to actual device responses. Experimental characteristics shown in the following were measured in the dark at 25°C, with the gate voltage applied through an Ag/AgCl reference electrode, soaked in a 0.1 M, NaCl solution electrolyte. Titration was performed by adding NaOH and HCl to the solution, while monitoring the pH value with a Crison 2002 pH-meter. Simulations take into account a realistic description of the actual doping profile, as well as fixed oxide charges and Si-SiO_2 interface traps. Figures 4 and 5 show the transfer characteristics at different pH values (at a given V_{DS}) and at different V_{DS} values (at a given pH), respectively. As can be seen, the agreement between simulated and measured curves is quite satisfactory and, in particular, the pH-dependent threshold shift is predicted accurately. A sensitivity of about 53 mV/pH can be extracted from the simulated V_{GS}(pH) data, in good agreement with both experimental results and literature data /14/.

3. FABRICATION PROCESS AND ELECTROCHEMICAL CHARACTERIZATION

As an example of ISFET fabrication technology, the ISFET-CMOS process developed at IRST is described in the first part of this section. Then, the main electrochemical parameters used to characterize ISFET's as pH sensors are defined and the main issues related to their measurement are discussed. Finally, results are presented from the electrochemical characterization of a chip, which has been especially-designed and fabricated to test the suitability of the IRST ISFET-CMOS technology for the production of ISFET-based pH sensors with on-chip read-out electronics /15/.

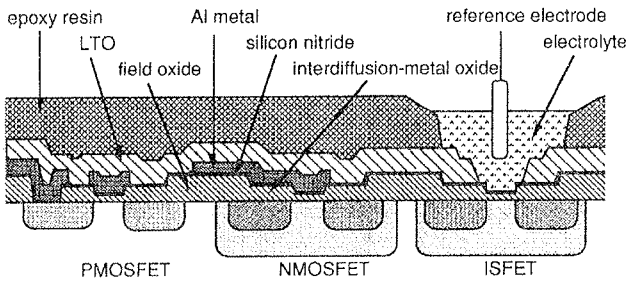

Fig. 6: Cross-sectional sketch of the n-channel ISFET and n- and p-channel MOSFET's produced by the ISFET-CMOS technology.

3.1 FABRICATION TECHNOLOGY

A summary of the process sequence is reported in Table 1, while a schematic cross-sectional view of the active devices produced is shown in Fig. 6. The basic sequence of the fabrication process consists of 13 photosteps and 7 implants, and closely resembles that of a conventional p-well, metal-gate, CMOS process. Some process steps have, however, been added or improved in order to get a higher flexibility and to make active

devices more resistant to the hostile conditions of the typical application environment. The threshold voltages of p- and n-channel devices, ISFET's included, are adjusted by separate implants. Channel-stop implants have been implemented for better device isolation, while, for improved ESD immunity, the natural inter-diffusion-metal oxide has been thickened by adding an undoped oxide, deposited at 712°C in an LPCVD system using TEOS. In addition, the breakdown voltage of source and drain junctions, as well as the source and drain contact resistances have been optimised in view of the CMOS integration. The gate dielectric is composed of 110 nm of thermally-grown SiO_2 and 100 nm of Si_3N_4, this latter providing the ion-sensitive layer. The Si_3N_4 layer is deposited at 775°C in an LPCVD system (ASM DRF 210), using ammonia and diclorosilane in a 4:1 flow ratio. Appropriate annealing steps are carried out to stabilize the layered oxide/nitride dielectric and to reduce the interface trap density. In order to minimize the fabrication process complexity the Si_3N_4/SiO_2 double layer is present on all transistors.

Table I: IRST ISFET-CMOS fabrication process outline

Substrate: CZ, (100), 8 ohm-cm, n-type Si
1st photostep: p-well 1st implant: Boron, 100 keV, $4.5x10^{12}$ cm^{-2}, through screenoxide p-well drive in: 1150°C, 15 h, dry
2nd photostep: p+ guard-ring 2nd implant: Boron, 120 keV, $1x10^{13}$ cm^{-2}, through screenoxide 3rd photostep: n-substrate active area 3rd implant: Phosphorus, 70 keV, $3x10^{12}$ cm^{-2}, through screenoxide field-oxide growth: 975°C, 9 h, steam, 1150 nm
4th photostep: define diodes
5th photostep: p^+-select 4th implant: BF_2, 80 keV, $5x10^{15}$ cm^{-2}, through screenoxide diode drive in: 975°C, 80 min, inert ambient
6th photostep: n^+-select 5th implant: Phosphorus, 80 keV, $5x10^{15}$ cm^{-2}, through screenoxide diode drive in: 1150°C, 1 h, inert ambient
7th photostep: define gate area 8th photostep: p-select 6th implant: BF_2, 50 keV, $1x10^{12}$ cm^{-2}, through sacrificial oxide
9th photostep: n-select 7th implant: Boron, 30 keV, $1x10^{12}$ cm^{-2}, through sacrificial oxide 10th photostep: p & n-select gate-oxide growth: 975°C, 30 min, dry, 30 nm LPCVD nitride deposition: 795°C, 30min, dry, 100 nm
11th photostep: contact opening Al sputtering deposition: 1200 nm
12th photostep: define metal LTO deposition: 430°C, 30 min, 500 nm
13th photostep: define overglass contact sintering: 400°C, 5 min

3.2 ELECTROCHEMICAL PARAMETERS

pH-sensitive insulators are characterized by three main parameters: sensitivity, drift rate, and hysteresis. These parameters appear to depend on the same fundamental phenomena occurring at the insulator-electrolyte interface and are therefore correlated to each other. Their values are influenced by the measurements procedure as well, and therefore suffer from lack of standardization, which often makes it difficult to quantitatively compare results published in the scientific literature.

Sensitivity is defined as the sensor output-voltage variation, induced by a unit change in the pH of the electrolytic solution. With the ISFET operated as in Fig. 2, for instance, pH-sensitivity can be measured by evaluating the slope of the V_{GS}(pH) linear regression. This parameter greatly depends on the chemical/morphological characteristics of the insulating layer exposed to the electrolyte.

ISFET operation has so far been assumed to be exempt from nonidealities, such as long-term drift and hysteresis. On the contrary, such phenomena have been found to affect all the main insulators used as pH-sensing surfaces, ultimately limiting the accuracy with which an ISFET can be used to measure pH.

Long-term drift is evidentiated by an irreversible output-voltage variation with time at constant pH. Despite no conclusive arguments about its origin has been presented yet, drift appears to be a consequence of the interaction of certain ions present in the electrolyte with either the surface or the bulk of the insulator /16/. An important characteristic of drift, which is common to all the main insulators used in ISFET's, is that the drift rate tends to rapidly decrease with time. This means that by waiting for a suffuciently long time, drift can be reduced to very low values. State-of-the-art Si_3N_4-ISFET's, for instance, show, after appropriate stabilization, drift of $0.1 \div 0.3$ mV/h.

A much more serious problem for the accuracy of the sensor is hysteresis, observed when an ISFET is exposed to consecutive upward and downward pH sweeps. Hysteresis is usually measured by evaluating the difference in the residues of the V_{ref} vs. pH linear regression after a pH closed loop. This phenomenon has been suggested to be a direct consequence of the presence in the ISFET time response to pH changes of a slow, delayed term following the immediate response /17/. While this latter lasts less than $1 \div 2$ min and accounts for more than 90% of the overall output variation, the time constant characterizing the slow response after a pH step is tipically in the order of $3 \div 4$ h. As a result, when the device is exposed to a periodic pH input, the output will be somewhat delayed relative to the input and thereby show a hysteresis. Due to the slow response, long-term drift has to be measured after appro-

priate stabilization time, in order to minimize the memory for previous pH change, avoiding any significant overlap between the long transient response and the actual device drift. As far as the origin of the slow response to pH changes (and therefore of hysteresis) is concerned, the most probable explanation, in the context of the site-binding model, is that a fraction of the sites responds more slowly to pH changes than those accounting for the immediate response This could in turn be due to imperfections in the insulator layer, such as roughness or microporosity, giving rise to sites located beneath the insulator surface. In the specific case of Si_3N_4, such interior sites might be secondary amines located close enough to the surface to be able to partecipate in a slow equilibrium with protons /17/. It is, in any case, widely recognized that more fundamental work, using surface physico-chemical characterization techniques, as well as improved phenomenological modelling, is needed for a complete understanding of the response of pH-sensing insulators employed in ISFET's.

3.3 AN ISFET-CMOS TEST CHIP

The test chip, a microphotograph of which is shown in Fig. 7, consists of three separate sections to cover the three main aspects involved in the ISFET-CMOS technology development, i.e. sensor optimization, techology evaluation, and testing of basic integrated-circuit blocks. With reference to Fig. 7, the top portion of the chip contains an ISFET and two matched, Al-gate, n-channel MOSFET's that can be used either coupled with the ISFET in a differential-stage configuration or as thermal sensor. The channel length and width of both ISFET and MOSFET's are 20 and 800 μm, respectively. The source and drain regions are extended to one end of the chip to the purpose of outdistancing the contacts from the gate region, thus easing lead attachment and packaging. The intermediate region of the chip is devoted to basic signal-processing circuit blocks and contains a differential stage and output stages of different types (CMOS, NMOS, and double-stage NMOS) and amplification factors. The bottom portion of the chip contains several test structures (such as differently sized capacitors, diodes, resistors, and transistors) devoted to technology evaluation.

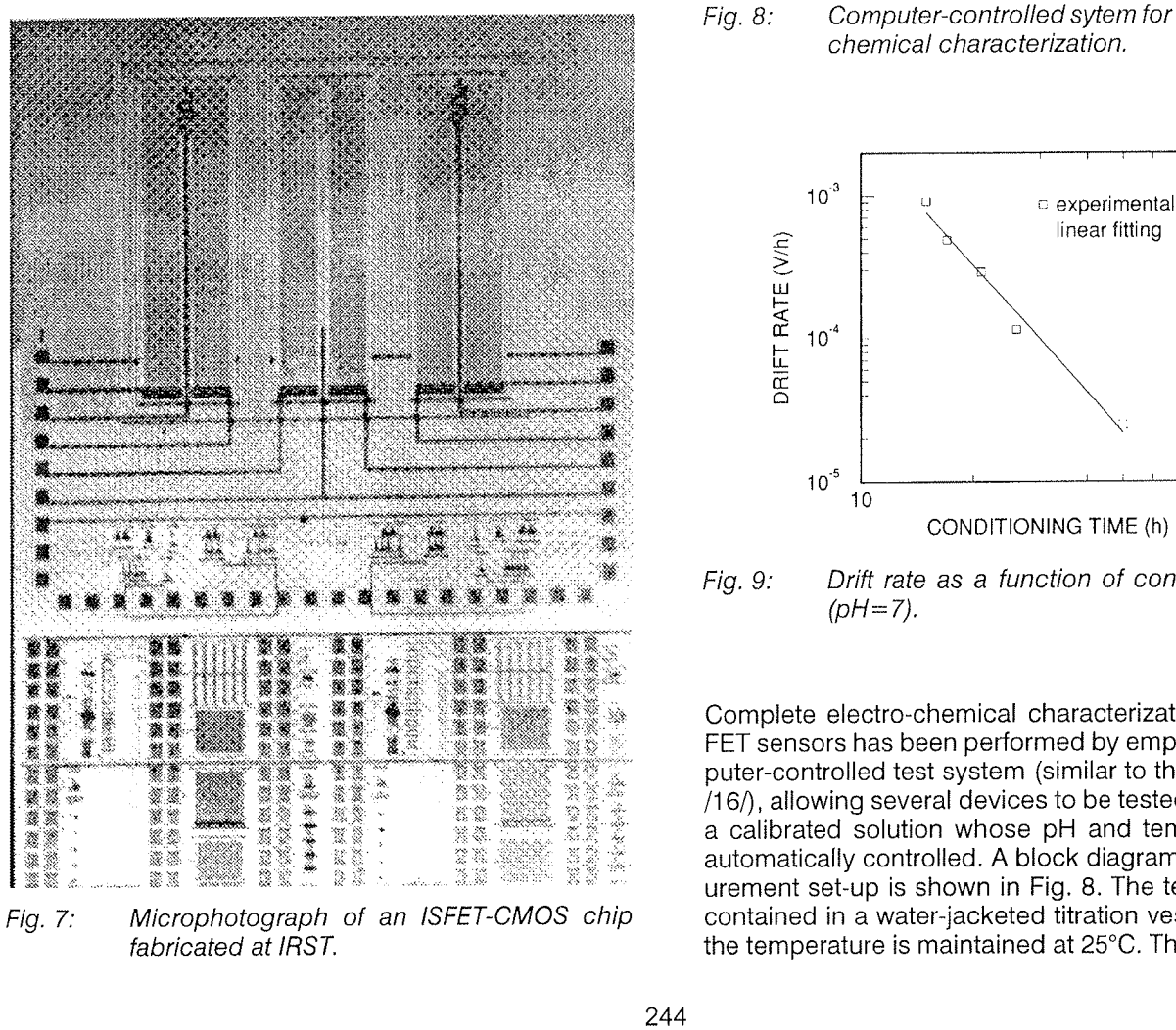

Fig. 7: Microphotograph of an ISFET-CMOS chip fabricated at IRST.

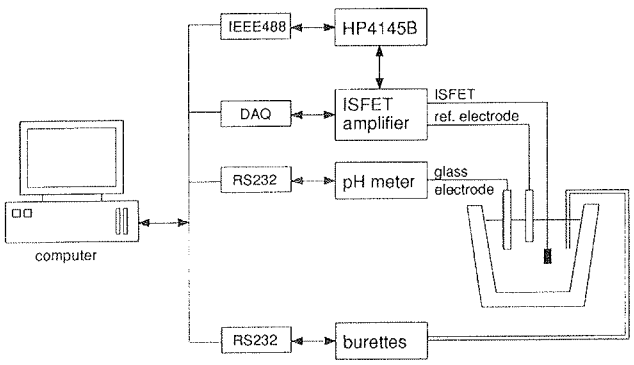

Fig. 8: Computer-controlled sytem for ISFET electrochemical characterization.

Fig. 9: Drift rate as a function of conditioning time (pH=7).

Complete electro-chemical characterization of the ISFET sensors has been performed by employing a computer-controlled test system (similar to that reported in /16/), allowing several devices to be tested in parallel in a calibrated solution whose pH and temperature are automatically controlled. A block diagram of the measurement set-up is shown in Fig. 8. The test solution is contained in a water-jacketed titration vessel, in which the temperature is maintained at 25°C. The pH is moni-

tored with a pH meter (CRISON 2002), while an Ag/AgCl electrode is used to provide the reference voltage for ISFET operation. Addition of acids and bases is carried out by means of two micro-burettes (CRISON 2031). The ISFET is connected to a feedback amplifier, shown in Fig. 2, allowing V_{DS} and I_{DS} to be set simultaneously by adjusting the gate voltage. This latter is measured by means of a data acquisition board (NI AT-MIO16L). A HP4145B semiconductor parameter analyzer is used to bias the ISFET and to measure currents. The burettes, the pH-meter, the data acquisition board, as well as the HP4145B are interfaced with a personal computer, controlling all the different phases of the characterization procedure. To this purpose, a package of C-language programs has been developed by exploiting the Lab-Window 2.0 environment. A typical test sequence includes: (i) encapsulation verification, (ii) measurement of the I_{DS} vs. V_{GS} characteristics; (iii) long-term drift evaluation; (iv) determination of pH sensitivity and hysteresis.

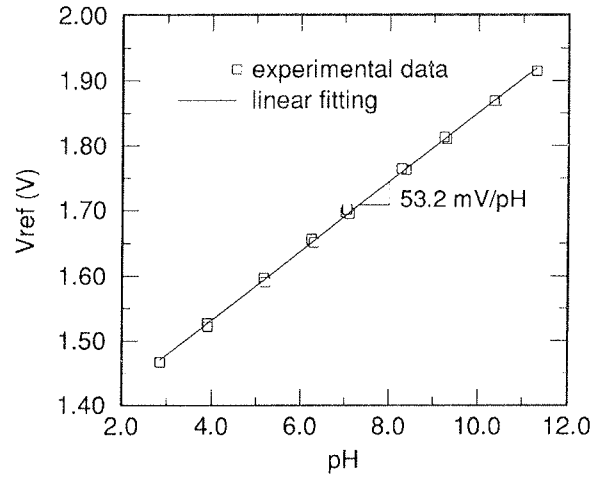

Fig. 10: Gate voltage (V_{ref}) as a function of pH. From the slope of the fitting line a sensitivity of 53.2 mV/pH is extracted

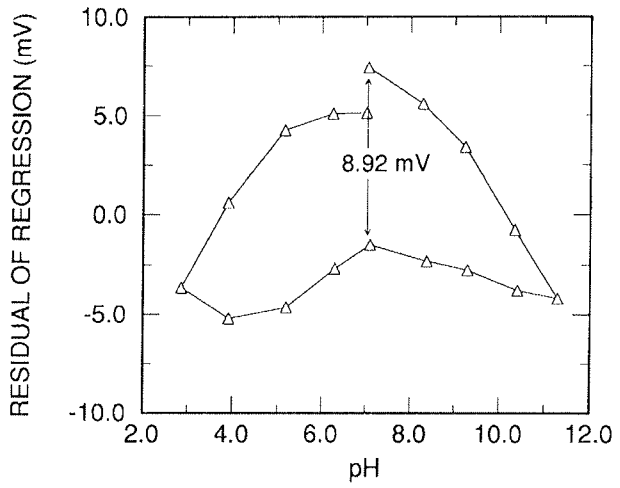

Fig. 11: Residues of the V_{ref} (pH) linear regression as a function of pH.

(i) To check the integrity of ISFET isolation, the leakage current flowing through the encapsulated device is measured, before and after the standard sensor conditioning (15 h at pH=7), by sweeping the reference electrode voltage from -3 to 3 V, while keeping source, drain and bulk terminals to ground /18/. ISFET with good-quality isolation shown leakage currents in the pA range throughout the wide reference-voltage interval adopted, whereas failures in the encapsulation are usually evidenced by exponetially growing leakage currents at voltages above certain threshold voltages. (ii) ISFET transfer characteristics are measured at constant pH (usually pH=7) and different V_{DS} voltages. Typical results are shown in Fig. 5. From the I_{DS} vs. V_{GS} characteristics electrical parameters, such as threshold voltage and transconductance, can easily be extracted. (iii) Drift rate is evaluated by monitoring the feedback-amplifier output, at constant temperature and pH (usually pH=7) for 1 h. ISFET's are immersed in the solution 12 to 50 h before drift measurement is started. In Fig. 9 results are reported, showing that the drift rate decreases markedly with time, reaching values comparable with the experimental error after conditioning times of 30÷40 h. (iv) Sensitivity and hysteresis are measured by changing the solution pH and monitoring the sensor output voltage. The electrolyte solution used is tipically a 0.1 M NaCl with low-concentraton buffers included to stabilize the pH reading. pH excursion begins at pH=7, where the ISFET is allowed to stabilize before the measurement starts. The pH is changed in steps of one unit down to 3, then stepped upwards to 7. After that, the sequence is repeated towards the basic extreme, which is usually pH=11. The time spent for each step is 6 min, the measurement of the output voltage being taken 4 min after each acid or base addition. Figure 10 and 11 show typical results of this experiment. V_{ref} is plotted against pH in Fig. 10, where the slope of the linear-regression line provide a pH sensitivity of 53.2 mV/pH. In Fig. 11, the residue of the linear regression is reported as a function of pH. The maximum amplitude of the hysteresis curve is measured at pH=7, yielding a value of 8.93 mV. Typical values of the different electrochemical parameters characterizing ISFET's fabricated at irst are summarized in Table 2.

Table II: Typical values of the main electrochemical parameters characterizing ISFET's fabricated at IRST.

PARAMETER	VALUE
sensitivity	51.0±1.3 mV/pH
hysteresis (3<ph<11)	11 ± 3 mV
linearity	0.9995
drift (after 50 h)	<500 μV/h

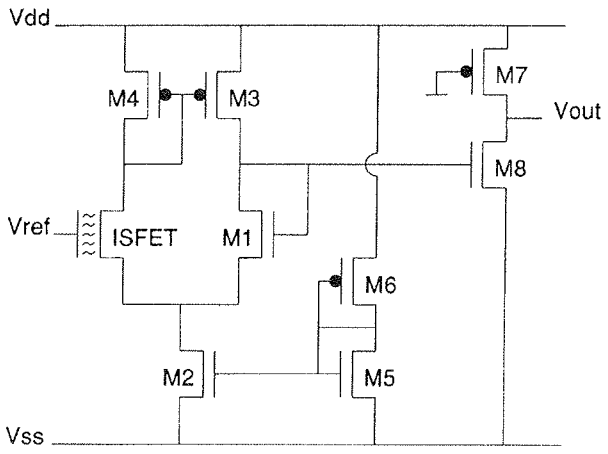

Fig. 12: Schematic of a differential stage with an ISFET as one of the input transistor and a CMOS output stage.

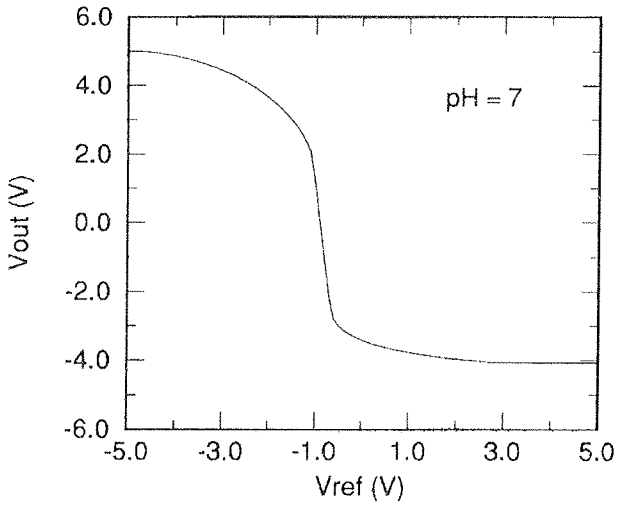

Fig. 13: Experimental transfer characteristic of the circuit in Fig. 12.

The functionality of all the circuit blocks present on the test chip has been verified both at wafer level and in packaged devices. As an example of testing in operating conditions, the transfer characteristic of a differential stage having an ISFET as one of the input transistors and a CMOS output stage is shown in Fig. 13. The schematic of the circuit is given in Fig. 12.

4. ION SELECTIVITY AND PACKAGING

In this section, the use of ISFET's to develop complete (bio)chemical sensors is discussed and the main technological drawbacks to overcome in order to fully exploit commercially the potentialities of ISFET's are reviewed. The everlasting problem of an efficient, reliable, low cost packaging procedure is then outlined.

4.1 DIRECTLY AND INDIRECTLY SENSING DEVICES

As stated previously, ISFET in its simplest form operates as a pH sensor, where its threshold-voltage shift depends upon the concentration of hydrogen ions in the electrolyte. The use of Si_3N_4 or Al_2O_3 or Ta_2O_5 as pH-sensitive insulator allows an almost linear response to be achieved. Selectivity can be provided by a semipermeable membrane covering the device. The use of different types of ion-selective polimeric membranes deposited on top of the gate insulator has led to the application of ISFET to detect other cations, such as Na^+ and K^+. The first report on ISFET covered with such membrane was published in 1975 /19/, when a potassium-sensitive ISFET was fabricated by covering the ISFET with a 300-μm thick plasticized PVC membrane. Following this first achievement, a variety of membrane covered ISFET's sensitive to calcium, sodium, ammonium, and other cations have been published. Moreover, the use of biological membranes such as enzimes has resulted in biosensors. Main problem with such approach to a specific chemical sensitivity is the membrane limited lifetime, mainly due to leaching of components and bad adhesion. To prevent leaching, membranes that are intrinsically rubbery, e.g. polysiloxanes, or photopolymerizable ion-selective membranes, e.g. methacrylate-type polimers, have been suggested and used. This latter approach might be suitable to mass production. However, to our knowledge, no successful on-wafer fabrication to produce low cost, highly reliable membrane covered ISFET's has so far been reported. To improve adhesion, a number of technological solutions have been proposed and tested. Since all the ion-sensitive membranes so far used are applied to the gate after encapsulation, membrane adhesion problems are closely related to ISFET packaging technology.

pH-sensitive ISFET's, as well as membrane-covered ISFET's, can be considered "directly sensing devices", since they directly provide a voltage output shift related to the specific ion concentration in the electrolytic solution. However, the practical application of ISFET's is not limited to the detection of ionic species only. It is also possible, in fact, to add an intermediate layer to the system to transduce, by a suitable auxiliary chemical reaction, a variation in a (bio)chemical variable into a corresponding variation of ionic species resulting from the auxiliary reaction, which can be directly sensed and measured. This is the way ISFET-based "indirectly sensing devices" operate. PCO_2-sensitive ISFET's /20, 21/ and ISFET-based enzime sensors /22/ are particularly relevant examples of such indirectly sensing approach. Also in these cases the use of an ISFET as the detecting element in a more complex chemical sensor is particularly attractive because of its small size and of the possibility to couple its ion-sensitive gate region to miniaturized flow-through chambers. Biomedical devices for extra-corporeal use often require flow-through chambers with a minimum internal volume, which allows for a small sample size and a fast response. Such structures can be recalibrated easily and regularly, thus solving the ISFET drift problem. The potential low cost of mass produced ISFET's is also of interest in the

development of biosensors, because the limited lifetime of biologically active intermediate sensing layers requires the use of cheap disposable sensors.

4.2 ENCAPSULATION AND PACKAGING

No sensor can be used in measurements without proper packaging. In fact, packaging should be considered as an integral part of the sensor design process. There is no unique and generally applicable packaging method for all the ISFET-based biochemical sensors. Each device works in a special environment and will have unique operational specifications. The packaging therefore will have to be designed to satisfy these conditions. Additional problems are encountered when ion-selective membranes are deposited on top of the ISFET transducer, i.e. the fixation of these membranes to the sensor and their compatibility with the packaging materials. Packaging should asssure: (i) electrical isolation of leads, sensor chip and electronics to prevent leakage; (ii) mechanical, optical and thermal protection to ensure structural integrity, dimensional stability and photo- or thermally-generated spurious signals; (iii) chemical isolation from the harsh external environment and, especially in case of biosensors, biocompatibility. Encapsulation materials interfacing with the environment should be inert and should not release toxic products during the sensing operation. It is evident that the final application of the sensor determines the packaging technology to be used. In this respect, the different approach in packaging methodology between disposable-type sensors (i.e. one-time use during relatively short time periods, with low price) and reusable sensors (i.e. repeatedly used, long time periods, higher price) has to be underlined.

With respect to the design and the development of ISFET-based biochemical sensors, the encapsulation and packaging remain an often underestimated aspect. Especially with the recently developed micromachining methods, totally new device realizations are conceivable, which offer improved long-term performance of the sensor. Also, a miniaturized reference electrode, which remains a necessary part of every electrochemical system, can possibly be integrated on chip with these techniques. Micromachining methods may also set the trend for future developments in miniaturized ion-sensor systems as, by using these techniques, complete biochemical analyzer systems based on arrays of specialized ISFET sensors integrated on a single chip can be envisaged.

5. APPLICATION EXAMPLES

The marketing opportunities of ISFET-based (bio)chemical sensors are first outlined. Then, two examples of systems recently developed at IRST for environmental applications are described.

5.1 MARKET PERSPECTIVES

Although the ISFET concept has existed for over 20 years, i.e. since the pioneering work of Bergveld in 1970 /1/, practical applications are still emerging only very slowly, in spite of the large research and development effort in the field. Two classes of practical problems have been and, at least partially still are, limiting factors in the commercial breakthrough and exploitation of biochemical sensors based on ISFET transducers: those which are inherent to the transducer itself, arising from limitations in materials and technologies used, and those which are common to the applications of any solid-state (micro)sensor, i.e. the need for an efficient encapsulation and packaging procedure, as stated previously, and the need for a stable, on chip micro-fabricated reference electrode.

Two application areas particularly suited for ISFET-based biochemical sensors that are becoming increasily important are the environmental monitoring and medical diagnosys. Both of these applications require quite sofisticated sensor systems and data processing methods. World-wide market for the various type of (bio)chemical sensors in these two fields was estimated to be 100 million US$ in 1990, with a predicted value of 700 to 800 million US$ for the year 2000. This market value forecast justifies the continuing research and development effort in the field. In the following, two different systems are described, aimed at the detection of microorganisms in water and of formaldehyde in air, respectively. Both systems exploit ISFET's as sensing elements. Full account of design, implementation, and testing of the two systems can be found /23/ and /24/, respectively.

5.2 ON-LINE DETECTION OF MICRO-ORGANISMS IN WATER

The system described in the following allows for the detection of living microorganisms by measuring the cell-induced acidification rate in micro-samples of water periodically drawn from the main stream under observation and conveyed to an especially-designed flow-through microchamber. This latter is encapsulated on top of the transducer chip. A sketch of the system block diagram is shown in Fig. 14. The fabrication technology and the layout of the sensor chip have already been described in Sec. 3.1 and 3.3, respectively. A Si_3N_4-ISFET and an Al-gate MOSFET form the input pair of a differential stage, followed by a CMOS output stage (see Fig. 12).

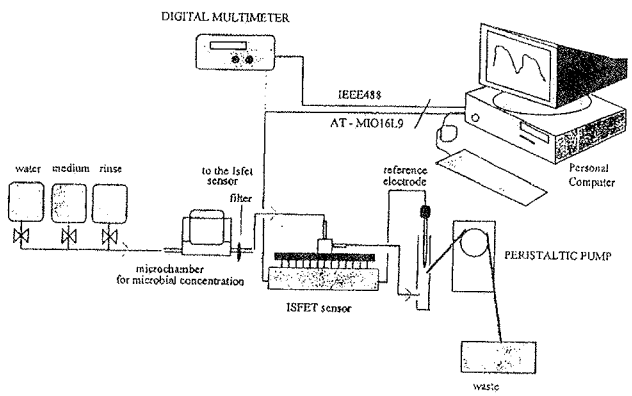

Fig. 14: Block diagram of the system for on-line detection of microorganisms in water.

The effectiveness of the system has been tested by means of two different experiments. In the first one, the system is fed with an F12 solution with known concentrations of bacteria (10^5 ml^{-1}, 10^6 ml^{-1}, 10^7 ml^{-1}). In the second, the system is fed with a sterile F12 solution, whereas the bacteria have previously been inserted into the syringe filter at the same different concentrations. The first experiment represents the simulation of an on-field measurement, the bacteria being contained in the flowing medium and accumulating in the filter during the measurement. In these conditions, the concentration of bacteria is fixed in the medium, while increasing in the filter. In the second experiment, which can be used to evaluate the system sensitivity, the microbial concentration inside the filter is constant. In both cases, the duration of the test is 60 min, the flow rate is 0.2 ml/min with an ON/OFF duty cycle of 10min/5min. Results from the first experiment are shown in Fig. 15 for different microbial concentrations. An increase in the total acidification detected by the system can clearly be observed. This is due to the fact that the total amount of bacteria inside the filter grows proportionally to the flow time. Figure 16 illustrates the results of the second experiment. As can be seen, the Δ pH is constant with time for microbial concentration of 10^5 ml^{-1} and 10^6 ml^{-1}, due to the fixed bacteria concentration inside the filter. At the microbial concentration of 10^7 ml^{-1}, the unexpected acidification change is probably related to variations in the metabolic state of the microorganism population.

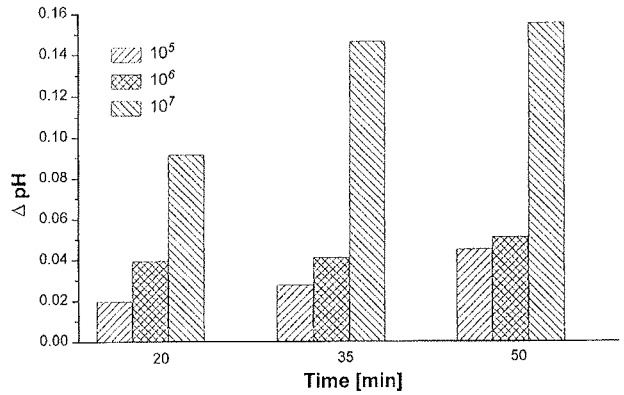

Fig. 15: pH variations for different microbial concentrations obtained in the first experiment.

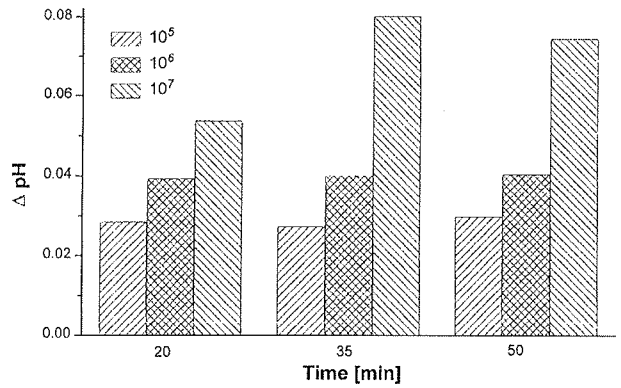

Fig. 16: pH variations for different microbial concentrations obtained in the second experiment.

5.3 POTENTIOMETRIC SAMPLING OF FORMALDEHYDE IN AIR

Formaldehyde, a suspected carcinom, is an automotive exhaust gas and an important chemical in the manufacturing of a variety of consumer products and in performance of medical services. Since conventional methods for the determination of formaldehyde (i.e., spectrophotometry, chromatography, or polarography) require expensive and bulky instrumentation with high power demand and well trained operators, a widespread observation of formaldehyde is prevented. In this context, the development of a portable, low-cost sensor for real-time monitoring of this gas-phase pollutant appears of large interest. In the following, a system for monitoring atmospheric formaldehyde is described, which exploits an ISFET in conjunction with an enzyme specific for this pollutant, namely formaldehyde dehydrogenase from *Pseudomonas putida* (FDDP). This enzyme, using oxidised nicotinamide adenine dinucleotide (NAD^+) as cofactor, catalyzes the oxidation of a molecule of formaldehyde with the parallel production of two protons which can be sensed by the ISFET.

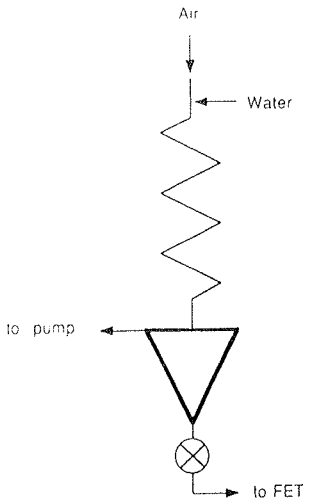

Fig. 17: Block diagram of the system for detection of formaldehyde in air.

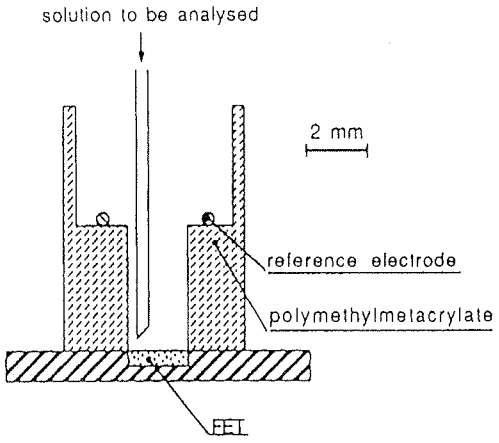

Fig. 18: Measurement cell containing the ISFET transducer.

The scheme of the sampling system is shown in Fig. 17. Formaldehyde is stripped from the atmosphere by pulling it concurrently with the scrubbing solution into a vertical coil. The scrubbing solution flows through the coil at the rate of 100÷200 µl/min, while the air is tipically sampled at 0.5÷1 l/min by a µP controller. The cell, a sketch of which is shown in Fig. 18, permits working volumes as low as 50 µl to be used and the analysing sample to be automatically replaced. The ISFET, whose fabrication technology and main electrochemical characteristics have already been described in Sec. 3.1 and 3.3, respectively, is operated with I_{DS}=100 µA, V_{DS}=300 mV, by means of a low-noise feedback amplifier, while the gate voltage is recored on an X-t chart recorder. ISFET active surface is covered by a membrane prepared by addition of glutaraldehyde (10 mg/l) to a solution of bovine serum albumin (40 mg/l), or by deposition of a solution of γ-aminoethyltriethoxysilane (22% in ethanol) followed by spin-off. FDDP is then covalently immobilized on the surface of the formed membrane by addition of N-(3-dimethylaminopropyl)-N'-ethylcarbodiimide hydrochloride, or alternatively added directly to the sampled solution. To improve detection limit and signal stability, a sodium pyrophosphate buffer in the concentration range 0.5÷2 mM is adopted.

As an example of system response, Fig. 19 shows the output of the ISFET transducer versus formaldehyde concentration. As can be seen, a linear response is measured up to 200 µM of formaldehyde. This behavior, which can appear in contrast with the Nernst law (according to which the response of the ISFET is proportional to the logarithm of the proton concentration), is a consequence of using a buffer at starting pH values close to the pK_a of the buffer itself /24/. A detection limit of 10 µM of formaldehyde in acqueous solution was estimated, corresponding, thanks to the enrichment factor introduced by the sampling system, to an athmospehric concentration in the ppb range.

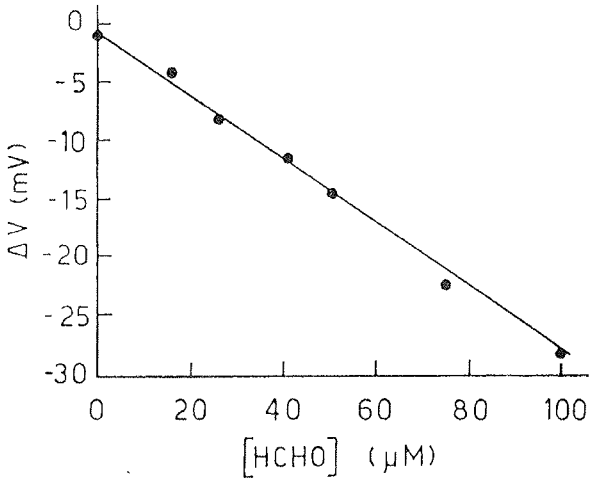

Fig. 19: Potentiometric response to increasing concentration of formaldehyde in the presence of FDDP.

6. CONCLUSIONS

The increasingly important and rapidly developing field of ISFET-based silicon integrated biochemical sensors has been addressed in this paper. ISFET basic operating principles, modelling and electrochemical characterization techniques have been reviewed. ISFET fabrication technology, mainly with reference to the ISFET-CMOS process developed at IRST, has been described. Finally, two examples of ISFET-based biochemical sensors for environmental monitoring applications have been presented.

References

/1/ P. Bergveld, "Development of an Ion-Sensitive Solid-State Device for Neurophysiological Measurements", IEEE Trans. Biomed. Eng., vol. 17, pp. 70-71, 1970.

/2/ P. Bergveld, "Development, Operation, and Application of the Ion-Sensitive Field-Effect Transistor as a Tool for Electrophysiology", IEEE Trans. Biomed. Eng., vol. 19, pp. 342-351, 1972.

/3/ I. Lundström et al. "Field Effect Chemical Sensors", in Sensors, a comprehensive survey, W. Göpel et al. eds., VHC, 1991.

/4/ M. Grattarola, G. Massobrio, and S. Martinoia, "Modelling H^+-Sensitive FETs with SPICE", IEEE Trans. on Electron Devices, vol. 39, no. 4, pp. 813-819, 1992.

/5/ D. E. Yates, S. Levine, and T. W. Healy, "Site-binding model of the electrical double layer at the oxide-water interface", J. Chem. Soc. Faraday I, vol. 70, pp. 1807-1818, 1974.

/6/ W. M. Siu, R. S. C. Cobbold, "Basic Properties of the Electrolyte-SiO_2-Si System: Physical and Theoretical Aspects", IEEE Trans. on Electron Devices, vol. 26, no. 11, pp. 1805-1815, 1979.

/7/ L. Bousse, N. F. De Rooij, and P. Bergveld, "Operation of Chemically Sensitive Field-Effect Sensors as a Function of the Insulator-Electrolyte Interface", IEEE Trans. on Electron Devices, vol. 30, no. 10, pp. 1263-1269, 1983.

/8/ C. D. Fung, P. W. Cheung, and W. H. Ko, "A Generalized Theory of an Electrolyte-Insulator-Semiconductor Field-Effect Transistor", IEEE Trans. Electron Devices, vol. 33, no. 1, pp. 8-18, 1986.

/9/ D. L. Harame, L. J. Bousse, J. D. Shott, and J. D. Meindl, "Ion-Sensing Devices with Silicon Nitride an Borosilicate Glass Insulators", IEEE Trans. on Electron Devices, vol. 34, no. 8, pp. 1700-1706, 1987.

/10/ P. R. Barabash, R. S. C. Cobbold, and W. B. Wlodarski, "Analysis of the Threshold Voltage and Its Temperature Dependence in Electrolyte-Insulator-Semiconductor Field-Effect Transitors (EISFET's)", IEEE Trans. on Electron Devices, vol. 34, no. 6, pp. 1271-1282, 1987.

/11/ L. Colalongo, G. Verzellesi, L. Quarella, D. Passeri, B. Margesin, P. Ciampolini, and M. Rudan, "Device-Level Analysis of Ion-Sensitive FETs", in Proc. of ISSDT'95, Berg-en-Dal, South Africa, pp. 112-114, November 1995.

/12/ G. Verzellesi, L. Colalongo, D. Passeri, B. Margesin, M. Rudan G. Soncini, and P. Ciampolini, "Numerical Analysis of ISFET and LAPS Devices", in Proc. of Eurosensors X, Lueven (Belgium), September 1996.

/13/ G. Baccarani, R. Guerrieri, P. Ciampolini, and M. Rudan, "HFIELDS: a Highly Flexible 2-D Semiconductor-Device Analysis Program", in Proc. of NASECODE IV, Dublin (Ireland), pp. 3-12, 1985.

/14/ H. Abe, M. Esashi, and T. Matsuo, "ISFET's Using Inorganic Gate Thin Films", IEEE Trans. Electr. Dev., vol. 26, no. 12, pp. 1939-1944, 1979.

/15/ A. Lui, B. Margesin, V. Zanini, M. Zen, G. Soncini, and S. Martinoia, "A Test Chip for ISFET/CMNOS Technology Development", in Proc. of the IEEE Int. Conf. on Microelectronic Test Structures, vol. 9, pp. 123-128, March 1996.

/16/ L. Bousse, H. H. Van Den Vlekkert, and N. F. De Rooj, "Hysteresis in Al_2O_3-gate ISFETs", Sensors and Actuators B, vol. 2, pp. 103-110, 1990.

/17/ L. Bousse et al., "Time Dependence of the Chemical Response of Silicon Nitride Surfaces", Sensors and Actuators B, vol. 1, pp. 361-367, 1990.

/18/ R. J. Huber, "Solid-State Chemical Sensors", J. Janata and R. J. Huber editors, Academic Press, 1989 Boston.

/19/ S.D. Moss, J. Janata and C.C. Johnson, Anal. Chem., vol. 47, p. 2238, 1975.

/20/ K. Shimada, M. Yano, K. Shibatani, Y. Komoto, M. Esashi, and T. Matsuo, J. of Med. Biol., Eng. Comp., vol. 18, p. 741, 1980.

/21/ B. H. van der Schoot, P. Bergveld, Sensors and Actuators, vol. 13, p. 251, 1988.

/22/ S. Caras and J. Janata, Anal. Chem., Vol. 52, p. 1935, 1980.

/23/ A. Cambiaso, S. Chiarugi, M. Grattarola, L. Lorenzelli, A. Lui, A. Maglione, B. Margesin, S. Martinoia, V. Zanini, "An H^+-FET Based System for the On-Line Detection of Micro-Organisms in Waters", in Proc. of the 8th. Int. Conf. on Solid-State Sensors and Actuators and Eurosensors IX, Stockholm (Sweden), June 1995, pp. 466-468.

/24/ F. Vianello, A. Stefani, M. L. Di Paolo, A. Rigo, A. Lui, B. Margesin, M. Zen, M. Scarpa, G. Soncini, "Potentiometric Detection of Formaldehyde in Air by an Aldehyde Dehydrogenase FET", to appear in Sensors and Actuators B, 1996.

/25/ L. Bousse, J. Shott, and J. D. Meindl, "A Process for the Combined Fabrication of Ion Sensors and CMOS Circuits", IEEE Electron Device Lett., vol. 9, no. 1, pp. 44-46, 1988.

/26/ J. A. Davis et al., J. Colloid Interface Sci., vol. 63, p. 480, 1978.

/28/ W. Smit et al., J. Colloid Interface Sci, vol. 7, p. 1, 1980.

/29/ J. Janata et al., Ion selective electrodes in anlytical chemistry, vol. 2, H. Freiser ed., Plenum, New York, 1980.

/30/ C. Cane, I. Gracia, A. Merlos, M. Lozano, E. Lora-Tamayo, and J. Esteve, "Compatibility of ISFET and CMOS Technologies for Smart Sensors" in Proc. 6th IEEE Int. Conf. Solid-State Sensors and Actuators (Transducers'91), San Francisco (USA), pp. 225-228, June 1991.

/31/ A. Sibbald, "Recent Advances in Field-Effect Chemical Microsensors", J. Molecular Electr., vol. 2, pp. 51-83, 1986.

/32/ H.S. Wong and M.H. White, IEDM Tech. Digest, pp. 658-661, 1988.

A. Lui, B. Margesin, M. Zen
Divisione Microsensori ed Integrazione di Sistema
38050 Povo (TN), Italy
tel. +39 461 314 537
fax: +39 461 314 591
G. Soncini, G. Verzellesi
Dipartimento di Ingegneria dei Materiali,
Universita di Trento, 38050 Mesiano (TN), Italy
tel. +39 461 882 423
fax: +39 461 881 977

Prispelo (Arrived): 16.9.1996 *Sprejeto (Accepted): 19.11.1996*